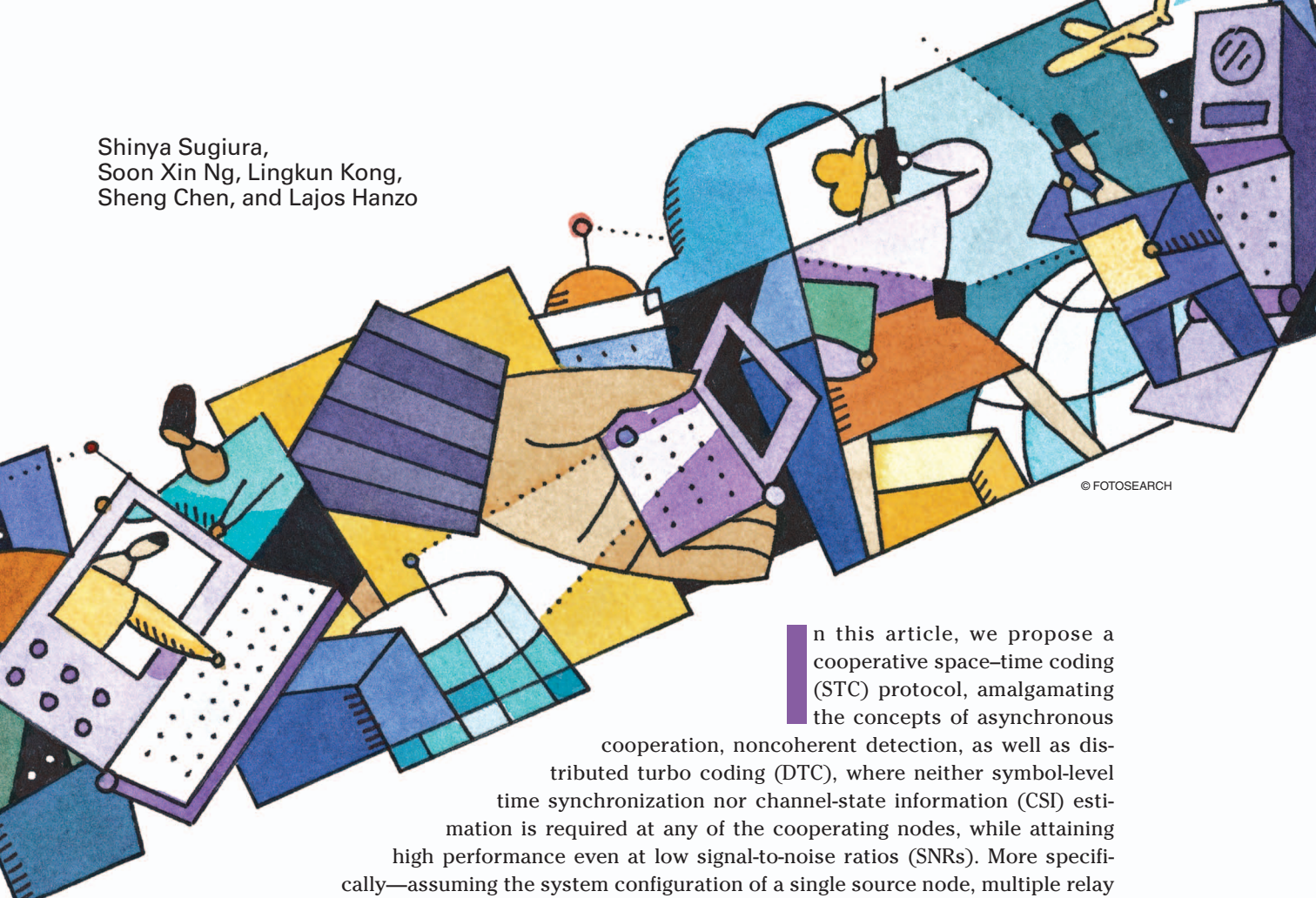


Shinya Sugiura,
Soon Xin Ng, Lingkun Kong,
Sheng Chen, and Lajos Hanzo



© FOTOSEARCH

In this article, we propose a cooperative space-time coding (STC) protocol, amalgamating the concepts of asynchronous cooperation, noncoherent detection, as well as distributed turbo coding (DTC), where neither symbol-level time synchronization nor channel-state information (CSI) estimation is required at any of the cooperating nodes, while attaining high performance even at low signal-to-noise ratios (SNRs). More specifically—assuming the system configuration of a single source node, multiple relay nodes, and a single destination node, each having a single antenna element (AE)—a practical cooperative differential space-time spreading (CDSTS) scheme is designed using interference rejection spreading codes, to eliminate the effect of synchronization errors between the relay nodes without the assistance of channel estimation or equalization. Furthermore, a set of space-time codewords are constructed based on differential linear dispersion codes (DLDCs), which allows our CDSTS system to support an arbitrary number of relay nodes operating at a high transmission rate because of its flexible design. Rather than using conventional single-relay-assisted DTCs, novel multirelay-assisted DTCs and a three-stage iteratively decoded destination receiver structure are developed for attaining a high-transmit

QUASI-SYNCHRONOUS COOPERATIVE NETWORKS

A Practical Cooperative Transmission Protocol

Digital Object Identifier 10.1109/MVT.2012.2193493

Date of publication: 10 December 2012

diversity order. In our simulations, the system parameters are designed using extrinsic information transfer (EXIT) chart analysis, followed by the characterization of the achievable bit error rate (BER) performance for various synchronization delay values, as well as for various diversity-multiplexing relationships in frequency-selective fast and/or quasi-static Rayleigh fading environments.

Introduction

Multiple-input, multiple-output (MIMO) techniques constitute promising solutions, where multiple AEs are employed at the transmitter and/or the receiver in conjunction with appropriate STC and modulation schemes. The exploitation of the spatial dimension provides a wireless system with an additional degree of freedom, hence facilitating the attainment of additional diversity gains, multiplexing gains, and beamforming gains. On the other hand, colocated MIMO AEs allow us to eliminate some of the performance limitations encountered in wireless communications. For example, the family of STCs constitutes an efficient class of diversity techniques that are capable of combating the time-varying fading effects of wireless channels.

However, the AEs of colocated MIMO systems typically suffer from spatially correlated large-scale fading imposed by the shadowing effects. For example, Figure 1 exemplifies the achievable BER performance of (2×1) -element STCs, namely, Alamouti's code portrayed in more detail, for example in [1, Section 7.3], assuming that the signals of the colocated AEs of the STC were correlated. More quantitatively, the spatial correlation factor ρ between the two channel elements was varied from $\rho = 0.1$ to 0.9 . Observe in Figure 1 that the diversity order of the colocated STC gradually eroded from two to one

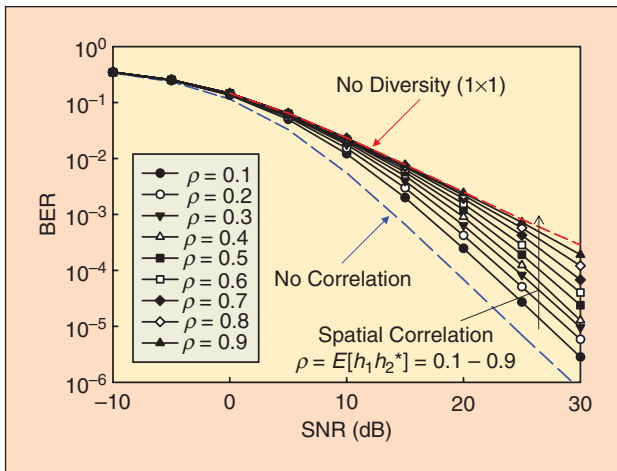


FIGURE 1 Comparison of colocated and cooperative MIMO systems, employing 2×1 Alamouti scheme, where spatial correlation $\rho_s = E[h_1 h_2^*]$ between the two channels was changed from $\rho_s = 0.1$ to $\rho_s = 0.9$, while the cooperative MIMO exhibited the no-correlation result.

THE FAMILY OF SPACE-TIME CODES CONSTITUTES AN EFFICIENT CLASS OF DIVERSITY TECHNIQUES THAT ARE CAPABLE OF COMBATING THE TIME-VARYING FADING EFFECTS OF WIRELESS CHANNELS.

upon increasing the correlation factor. Further to the effects of the above-mentioned spatial correlation, the MIMO transceiver may suffer from channel estimation errors. Figure 2 shows the achievable BER performance of the two space-time diversity schemes, employing both coherent and noncoherent receivers, where the (2×1) -element STC of Alamouti was employed for the coherently detected scheme, while the (2×1) -element differentially encoded orthogonal STBC (DOSTBC) scheme characterized in [1, Section 8.3] was used for the noncoherent scheme. To characterize the effects of the CSI estimation errors associated with coherent detection, we superimposed Gaussian noise having a variance of σ_H^2 on each channel tap h_i ($i = 1, 2$), for modeling the effects of channel estimation errors, while varying the variance σ_H^2 from $\sigma_H^2 = 0.01$ to $\sigma_H^2 = 0.3$. The BER curve of the differentially encoded scheme exhibited the well-known 3 dB performance loss compared with that of Alamouti's code assuming perfect CSI. When the effects of CSI errors are considered, the BER curves of the coherent detection aided scheme exhibited an error floor, and its performance was severely degraded upon increasing the channel estimation error variance σ_H^2 . Therefore, despite its 3 dB SNR disadvantage arising from differential encoding, noncoherent detection was found to outperform its realistically modeled coherent counterpart suffering from CSI estimation errors.

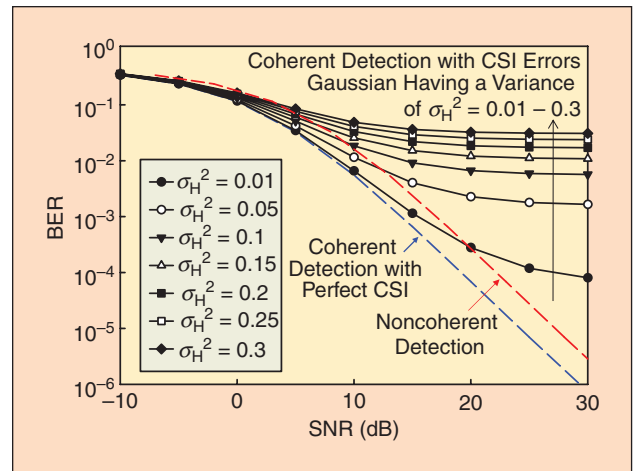


FIGURE 2 Achievable BER performance of coherent and noncoherent STC, characterizing the effects of channel estimation errors, where the (2×1) -element BPSK-modulated Alamouti scheme and the (2×1) -element BPSK modulated DOSTBC schemes were compared.

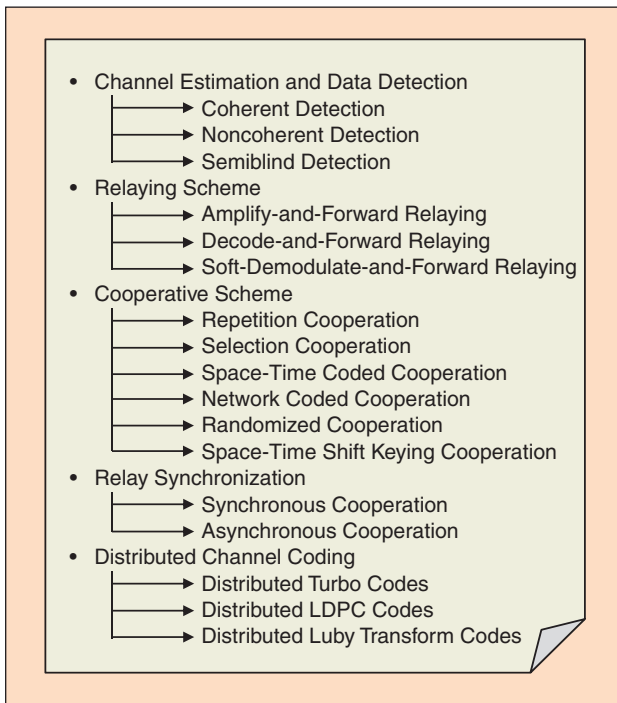


FIGURE 3 Design options and classification of cooperative communication techniques.

In recent years, cooperative STC schemes [2] as well as the suite of related techniques listed in Figure 3 were proposed, where a collection of single-antenna-aided nodes act as a virtual antenna array, having widely separated distributed AEs. This spatially dispersed mobile-station based distributed MIMO architecture enables us to exploit the maximum achievable diversity order, while avoiding the detrimental effects of the colocated MIMO's interantenna correlation, which is shown in Figure 1. Additionally, several CDSTC schemes [3] have been developed to combat the above-mentioned channel estimation error-related problem. More specifically, since it is a challenging task to acquire accurate CSI for both the source-relay (SR) and/or for the relay-destination (RD) links for a rapidly changing topology of vehicles traveling at high velocities, in recent years, noncoherent detection techniques attracted substantial attention.

On the other hand, the aforementioned cooperative STC schemes [2], [3] have exploited the assumption of perfect symbol timing synchronization between the cooperating nodes, which is typically an unrealistic assumption, considering the rapidly changing topology of the relay nodes. Since the resultant time synchronization errors impose a significant performance degradation as noted in [4], asynchronous cooperation schemes were investigated in [5] and [6], which are predominantly based on either equalization techniques [5] or on the employment of guard interval-aided multicarrier transmission schemes [6]. It should be noted that these asynchronous cooperation schemes assumed having

perfect CSI and/or delay information at the destination node, which was invoked to compensate for the dispersive channel's effects and for the resultant orthogonality degradation of the transmitted STC at the cost of an additional complexity. In this contribution, a practical CDSTC scheme is designed using interference rejection spreading codes, namely, loosely synchronous (LS) codes [7], because the LS codes are capable of eliminating the effects of multiuser interference (MUI) even with the use of single-user receivers, i.e., without relying on elaborate interference-cancellation techniques.

Moreover, the DTC philosophy was presented in [8] and [9], where the turbo-coding principle [10] was applied to a single-relay-assisted cooperative system. While, in general, cooperative STCs have the capability of achieving the maximum attainable diversity order in the high SNR regime, the DTC aims for achieving an additional turbo processing gain, and therefore, it is particularly suitable for operation at low SNRs. Here, we note that most of the previous DTC schemes proposed in the open literature [8], [9] are based on a two-stage parallel-concatenated arrangement assisted by a single relay node, assuming that there is a perfect link between the cooperating nodes. More recently, a sophisticated three-component distributed turbo trellis-coded modulation scheme was proposed in [11], also assuming the assistance of a single relay node.

Against this background, the novel contributions and rationale of this article are as follows:

- 1) We present a cooperative STC protocol, intrinsically amalgamating the concepts of asynchronous cooperation, of noncoherent detection as well as of DTC, which is capable of achieving beneficial spatial-diversity and iterative-processing gains. More specifically, assuming the configuration of multiple relay nodes, which experience realistic synchronization errors among them as well as independent path-loss and Rayleigh fading effects, in our CDSTC scheme, a multirelay-assisted three-stage DTC is employed to take maximum advantage of the potentially available relay nodes, unlike the family of conventional single-relay-assisted DTCs [8], [9], [11]. We emphasize that the asynchronous cooperation technique employed plays a beneficial role.
- 2) The STC blocks of our CDSTC are constructed based on DLDCs [12], which have the capability of striking a flexible diversity versus multiplexing tradeoff, depending on the number of relay nodes as well as on the target transmission rate. Additionally, as mentioned above, we invoke the multiple-relay-assisted DTC technique, to conceive a practical forward error correction (FEC)-assisted cooperative system.
- 3) A unity rate code (URC) and a recursive systematic convolutional (RSC) code are incorporated into our

OUR MULTIRELAY-ASSISTED DTC HAS THE POTENTIAL TO EXHIBIT A BETTER PERFORMANCE THAN THOSE OF THE CONVENTIONAL SINGLE-RELAY-ASSISTED DTCs.

Source Model

During the broadcast phase-I, the source node transmits its differentially encoded signals to the corresponding M relay nodes as well as to the destination node. As shown in the upper left corner of Figure 4, the source node first channel-encodes the source bits $b(i)$ using a half-rate RSC code and then interleaves the channel-encoded bits by using the source-specific interleaver Π_s . Furthermore, the interleaved bits are further encoded by a recursive URC (the role of the URC is to impose an infinite impulse response, which improves the achievable iterative decoding performance by efficiently spreading the extrinsic information without requiring a longer interleaver; more specifically, as detailed in [14], a recursive inner code is necessary for the sake of maximizing the interleaver gain and for avoiding the formation of a BER floor, when employing iterative decoding), and then the coded bits are input to the differential phase-shift keying (DPSK) mapper block. Finally, the DPSK-modulated symbols $c(k)$ are spread using the source-specific direct sequence spreading code $\xi_s(t)$, having the code length of L_s and the chip durations of T_c .

Under the condition of frequency-selective Rayleigh fading channels having a maximum number of resolvable paths L_p , the time-domain signals $y_m(t)$ received at the m th relay node, and the destination node $y_{sd}(t)$ are expressed, respectively, as

$$y_m(t) = \sqrt{P_s G_{sr}} \sum_{k=0}^{N_M-1} \sum_{l=1}^{L_p} h_{sr_m}^{(l)} c(k) \xi_s(t - kL_s T_c) + n_m(t), \quad (1)$$

$$y_{sd}(t) = \sqrt{P_s} \sum_{k=0}^{N_M-1} \sum_{l=1}^{L_p} h_{sd}^{(l)} c(k) \xi_s(t - kL_s T_c) + n_d(t), \quad (2)$$

where $h_{sr_m}^{(l)}$ and $h_{sd}^{(l)}$ are the corresponding Rayleigh fading coefficients associated with the l th path, while n_m and n_d are the noise components having a zero mean and a variance of $N_0/2$ per dimension. Furthermore, N_M indicates the number of modulated symbols. Here, the SNRs at the relay nodes, namely SNR_{sr} , and at the destination node SNR_{sd} have the relation of $\text{SNR}_{sr} = \text{SNR}_{sd} + 10 \log_{10}(G_{sr})$ expressed in decibels because of the geometrical power-gain effect [11]. Furthermore, the transmission rate of the phase-I R_s is given by $R_s = \frac{r}{2}$ b/symbol, where r is the number of b/symbol for the DPSK modulation scheme employed.

Relay Model

During the cooperative phase-II, the M relay nodes, which are shown in the lower left corner of Figure 4, implement the decode-and-forward CDSTC transmission scheme based on the DLDC-coded STS concept, where each of the M relay nodes uses all the M spreading codes according to the DSTS principle [15]. The M spreading codes have a code length of L_R . Letting the m th relay node be the node of interest, the received signals $y_m(t)$ are first despread by the source node's spreading code $\xi_s(t)$, and then iteratively decoded according to the turbo principle. Next, the estimated bits $\hat{b}(i)$ are interleaved and coded by the interleaver Π_R and the URC encoder, which are common for the associated M relay nodes. Then, the coded bits are mapped to DLDC blocks [12], which are represented by $S^{(k)} = [s_{ij}^{(k)}] \in \mathbb{C}^{M \times M}$, where $s_{ij}^{(k)}$ indicates the i th-row and j th-column element of the codeword $S^{(k)}$ and k is the block index. Note that $\mathbb{C}^{M \times M}$ denotes complex-valued matrix space, having the size of M rows and M columns. Here, Q BPSK symbols are multiplexed in each of the codewords $S^{(k)}$. It should be emphasized that the DLDC has the capability of striking a balance between the attainable diversity and multiplexing gain [12], enabling us to generate a set of M codewords while having a multiplexing order Q , without exhibiting a substantial information rate loss in comparison to the theoretical upper bound. This high degree of freedom enables the flexible adjustment of the number of cooperating relay nodes and the resultant phase-II throughput, depending on the rate of change in the network topology and the propagation environment.

Instead of arranging for each relay node to transmit each row of the DLDC codeword $S^{(k)}$ during M symbol durations in the conventional way [2], here we apply the concept of STS [15] during the phase-II transmissions using the M spreading codes seen in the lower left part of Figure 4. This operation assists the destination receiver to rearrange the received DLDC space-time codeword, hence eliminating the effect of synchronization errors between the relay nodes, provided that the spreading sequences have ideal cross-correlation properties. To be specific, the m th relay node spreads each component of the m th row in $S^{(k)}$ using a different spreading code for each component, and transmits the linear combination of the spread symbols in a concerted action with the other relay nodes, as closely synchronized as possible. Therefore, the time-domain signals $y_{rd}(t)$ received at the destination node during phase-II, shown in the right corner of Figure 4, is represented by

$$y_{rd}(t) = \sqrt{\frac{P_R G_{rd}}{M}} \sum_{k=0}^{N_B-1} \sum_{l=1}^{L_p} \sum_{m=1}^M \sum_{j=1}^M h_{rd_m}^{(l)} s_{m,j}^{(k)} \xi_j(t - kL_R T_c - \tau_{m,l}) + n_d(t), \quad (3)$$

where $h_{rd_m}^{(l)}$ is the Rayleigh channel coefficient between the m th relay node and the destination node, associated with the l th path, while $\tau_{m,l}$ is the delay component corresponding to the m th user and the l th path. Furthermore, $\xi_j(t)$ is the normalized signature sequence of the j th spreading code. Note that the corresponding transmission rate R_R of phase-II is given by $R_R = Q$ b/symbol. Similar to the SR SNR of SNR_{sr} , the RD SNR of SNR_{rd} and the source-destination SNR of SNR_{sd} have the relation of $\text{SNR}_{rd} = \text{SNR}_{sd} + 10 \log_{10}(P_R G_{rd}/P_S)$ in decibels.

At the destination node shown at the right of Figure 4, the source bits are iteratively detected based on the signals $y_{sd}(t)$ in (2) received during phase-I as well as the signals $y_{rd}(t)$ in (3) received during phase-II, which is detailed in the following section.

Three-Stage Iterative CDSTS Detector Structure

We present the destination receiver's structure for our CDSTS scheme, where a three-stage iterative decoding algorithm is employed, as illustrated in the right corner of Figure 4. For ease of treatment, we refer to the DPSK demapper, the URC decoder, and the RSC decoder of phase-I as an inner decoder, while the DLDC demapper and the URC decoder of phase-II are considered as an outer decoder. To be specific, the soft-input soft-output (SISO) decoders at the receiver iteratively exchange soft extrinsic information L_i^e in the form of log likelihood ratios (LLRs). At the inner decoder of Figure 4, the destination receiver decodes the signals broadcast from the source node during phase-I, to output the extrinsic LLR $L_1^e(i)$. The same procedure is followed by the relays' iterative decoders seen in Figure 4, with the sole difference that the RSC decoder block of the above-mentioned inner decoder can make use of the a priori information $L_1^q(i)$ gleaned from the outer decoder. The number of inner iterations between the two decoders within the inner decoder is represented by I_{Di} .

By contrast, at the outer decoder of Figure 4, the destination receiver first despreads the signals, which are received during phase-II. We note here that at this despread stage the effects of the synchronization errors between the relay nodes are eliminated. Then, the DLDC demapper produces soft information, where a conventional low-complexity linear MIMO decoder can be employed because of the linearization operation of [12]. Then, the resultant soft information is input to the URC decoder of Figure 4 to output the extrinsic LLR $L_3^e(i)$ of the outer decoder. Furthermore, the soft LLRs are iteratively exchanged between the inner decoder and the outer decoder, where the associated number of outer iterations is denoted as I_{Do} . Note that in this three-stage iterative decoding process, the total number of iterations is given by $(I_{Di} \times I_{Do})$. Finally, the estimated bits are

THE DESIGN OF FORWARD ERROR CORRECTION SCHEMES EMPLOYED AT THE SN AND THE RNS ARE OPTIMIZED USING TWO-DIMENSIONAL EXIT CHARTS.

calculated from the LLRs $L_1^q(i)$ and $L_1^e(i)$ using the hard-decision operation.

Interference Rejection Spreading Codes Having an Interference-Free Window

In our CDSTS scheme, the effects of asynchronous relay nodes are eliminated under the ideal assumption that the despreading operation at the destination receiver is capable of sufficiently suppressing both the asynchronous MUI as well as the multipath-induced intersymbol interference (ISI). This indicates that low cross-correlations as well as autocorrelations are required for the spreading codes employed. However, the conventional spreading codes, such as Walsh codes and Gold codes, normally suffer from both MUI and from multipath interference (MPI) due to the non-negligible auto- and/or cross-correlation values. To this end, we employ here the above-mentioned LS codes as the spreading codes in our CDSTS system. The family of LS codes exhibits a so-called interference-free window (IFW), resulting in zero ISI and zero multiple-access interference, provided that the maximum delay of the asynchronous transmissions including all MPI components is within the width of the IFW.

As detailed in [7], the parameter-based notation of LS codes is given by $\text{LS}(N_{LS}, P_{LS}, W_0)$, where N_{LS} is the length of the constituent orthogonal complementary code set, P_{LS} is the dimension of the Walsh-Hadamard matrix used for generating members of the code-family, and W_0 is the width of the IFW, which are used to design the desired LS code. As a result, we can generate P_{LS} LS codes having an IFW of at least $\min\{N_{LS} - 1, W_0\}$ chip durations, where the corresponding code length of the LS codes is $L = N_{LS} P_{LS} + 2W_0$. Owing to space-limitations, the detailed method of creating the LS code is omitted, which is available in [7].

EXIT Chart Analysis

We investigate the effects of diverse system parameters on our CDSTS system using EXIT charts [13]. Here, the number of source nodes allocated to each time slot is set to $N_c = 4$. Let us define here the equivalent transmit SNR ρ as $\rho = (P_S + P_R)/N_0$, which relates the total source-power P_S plus relay-power P_R to the noise-power N_0 at the receiver. Additionally, we consider frequency-selective block-fading Rayleigh channels, where the channel coefficients can be regarded as constants during two DLDC block durations, while the number of

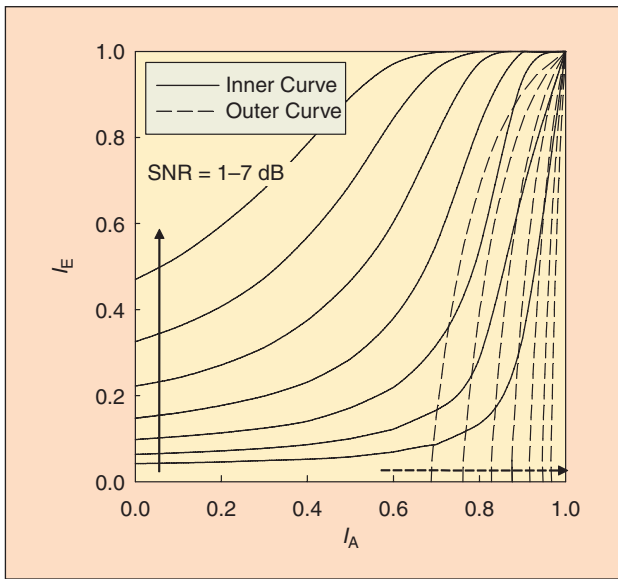


FIGURE 5 The EXIT curves of the inner decoder and outer decoders of our CDSTS system seen in Figure 4, supporting $N_c = 4$ source nodes in each time slot and employing DQPSK modulation at each source nodes and BPSK multiplexing associated with $Q = 2$ per DLDC block at the corresponding $M = 2$ relay nodes. The equivalent transmit SNR was varied from SNR = 1 to 7 dB, while the maximum synchronization delay was $\tau_{\max} = 3T_c$.

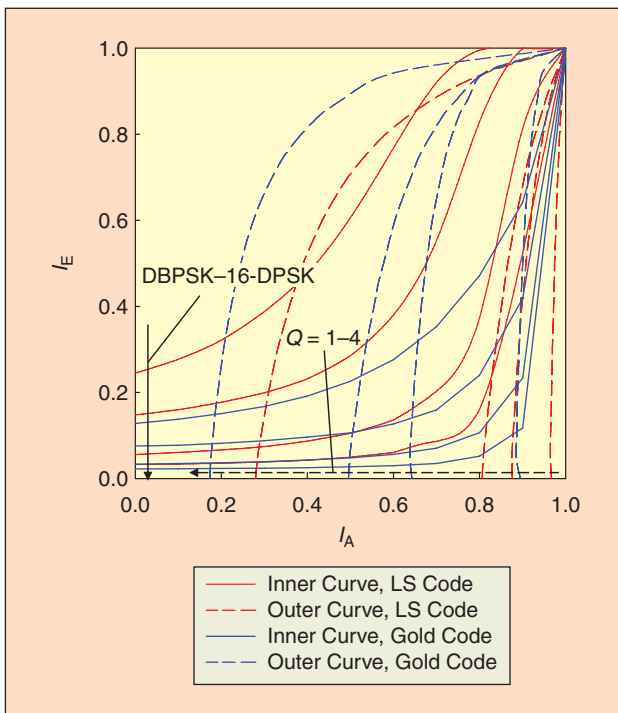


FIGURE 6 The EXIT curves of the inner and outer decoders of our CDSTS system seen in Figure 4, comparing different modulation schemes, such as DBPSK, DQPSK, 8-DPSK, and 16-DPSK for the source nodes as well as for DLDC multiplexing factors of $Q = 1, 2, 3,$ and 4 for the relay nodes, while an equivalent transmit SNR = 4 dB and a maximum synchronization delay of $\tau_{\max} = 3T_c$.

resolvable paths L_p as well as the number of rake combiner fingers ν is four.

First, we investigated the decoding characteristics of the destination receiver of Figure 4 in our CDSTS system, where each source node was assisted by $M = 2$ relay nodes and $Q = 2$ BPSK symbols were multiplexed per each DLDC codeword. We assumed that the each node's geometrical relationship, defined in "System Overview," was given by $G_{sr} = 8$ and $G_{rd} = 2$. Furthermore, the LS(8,4,7) and LS(8,8,7) codes were preassigned for the source and relay nodes, respectively. Figure 5 shows the EXIT curves of both the inner decoder and the outer decoder, where the transmit SNR was varied from SNR = 1 to 7 dB in 1 dB steps, while satisfying the maximum synchronization delay range of $\tau_{\max} = 3T_c$. Furthermore, a half-rate RSC code having the octally represented generator polynomials of $(g_r, g) = (7, 5)_8$ was employed as our channel encoder at the source nodes. As we can see from Figure 5, upon increasing the transmit SNR, the open EXIT tunnel between the EXIT curves of the inner and outer decoders becomes wider, potentially leading to a fast convergence of the iterative process, although the Monte-Carlo-simulation-based bit-by-bit decoding trajectories are not shown here.

Furthermore, in Figure 6, we investigated the effect of different modulation orders for both the source and relay nodes at the equivalent transmit SNR of 4 dB, where we considered DBPSK, DQPSK, 8-DPSK, and 16-DPSK modulation schemes for the source nodes as well as the DLDC multiplexing factors of $Q = 1, 2, 3,$ and 4 for the relay nodes. Here, we also employed Gold codes as the benchmark spreading codes of the LS codes, noting that Gold codes constitute well-known spreading sequences having relatively good asynchronous cross-correlation properties. Observe in Figure 6 that our LS code-based CDSTS scheme created open tunnels between the inner and outer EXIT curves in the cases of low-modulation orders, such as DBPSK, DQPSK, and 8-DPSK, as well as DLDC multiplexing factors of $Q = 1, 2,$ and 3 . By contrast, the employment of 16-DPSK or of $Q = 4$ gives rise to the closure of the EXIT tunnel. On the other hand, as shown in Figure 6, the EXIT curves of the Gold code-based CDSTS arrangement did not exhibit an open tunnel for every combination of the inner EXIT curve and the outer EXIT curve. This is because the LS codes' IFW successfully eliminated the effects of the synchronization errors between the relay nodes, while suppressing the MUIs imposed by the other source and relay nodes, also having synchronization errors. To be specific, upon increasing the modulation order for the source or the relay nodes, the corresponding EXIT tunnel becomes narrower or closed for both the LS and Gold spreading codes, implying that as expected, a higher SNR is required to attain a good BER performance in comparison to the lower modulation

orders. Additionally, we note that the outer decoder's EXIT curves in Figures 5 and 6 did not emerge from the origin of the coordinate system at $(I_A, I_E) = (0, 0)$, which is different from that of a typical serially concatenated turbo-coded system. This is because the source-relay-destination links of our CDSTS system seen in Figure 4 may be viewed as a parallel-concatenated branch, rather than that of the classic serially concatenated turbo-coding scheme. Hence, the corresponding inner decoder's EXIT curve acted similarly to that of parallel-concatenated turbo coding, which does not emerge from the point of $(I_A, I_E) = (0, 0)$.

Performance Results

The basic system parameters employed in our simulations are listed in Table 1, which we derived using our EXIT chart analysis of the previous section. A DQPSK modulation scheme and an interleaver Π_S having the length of 20,000 b were employed at the N_C source nodes, each of which was assisted by $M = 2$ relay nodes employing a DLDC multiplexing factor of $Q = 2$ and an interleaver Π_S having a length of 10,000 b. The number of iterations at each relay node I_R was set to $I_R = 5$, while the number of inner and outer iterations at the destination node was given by $I_{Di} = 2$ and $I_{Do} = 5$, respectively. Furthermore, the maximum synchronization delay τ_{\max} was set to $\tau_{\max} = 3T_c$.

Here, the total transmission rate of our CDSTS R_{total} was given by $R_{\text{total}} = L_S / (L_S/R_S + L_R/R_R)$ [b/symbol], where L_S and L_R are the code lengths of the spreading codes during phase-I and phase-II, respectively, and the rate R_{total} was normalized by the phase-I code length L_S . Based on these relationships, the transmission rate of our CDSTS was given by $R_{\text{total}} = 0.54$, while for instance that of the DBPSK-modulated noncooperative scenario was $R_S = 0.5$.

Figure 7 shows the achievable BER performance of our LS code-aided and Gold code-aided CDSTS schemes, where the maximum synchronization delays τ_{\max} were set to $\tau_{\max} = 3T_c, 6T_c$, and $9T_c$, while having $L_p = 4$ resolvable paths and $\nu = 4$ rake combiner fingers. It can be seen from Figure 7 that the BER curve of our LS code-based CDSTS system recorded for the case of $\tau_{\max} = 3T_c$ exhibited a good BER performance, as expected on the basis of the EXIT chart analysis of Figure 5 in the previous section. On the other

TABLE 1 Basic system parameters.

Source node	Number of source nodes N_C per time slot	4
	Modulation scheme	DQPSK
	Interleaver block length of Π_S	20,000 b
	Spreading codes	LS codes of LS(8,4,7)
	Outer channel code	RSC with generator polynomials $(7,5)_8$
Relay node	Precoder code	URC $G(D) = 1/(1 + D)$ with a delay element D
	Power allocation P_S	0.5
	Number of relay nodes per source node M	$M = 2$
	Modulation scheme	BPSK-modulated DLDC [12]
	DLDC's multiplexed factor Q	$Q = 2$
	Interleaver block length of Π_R	10,000 b
	Spreading codes	LS codes of LS(8,8,7)
	Precoder code	URC $G(D) = 1/(1 + D)$ with a delay element D
	DPSK demapper	Soft demapper
	Number of iterations I_R	5
Destination	Power gain of SR links G_{sr}	8
	Power allocation P_R	0.5
	DPSK demapper	Soft demapper
	DLDC demapper	MMSE-based soft interference cancellation
	Number of inner iterations I_{Di}	2
	Number of outer iterations I_{Do}	5
	Power gain of RD links G_{rd}	2

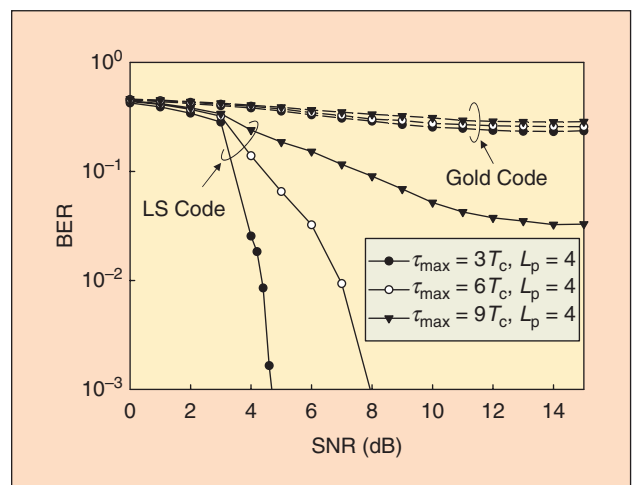


FIGURE 7 Achievable BER performance of our LS code-aided CDSTS and the Gold code-aided CDSTS schemes, comparing the maximum synchronization delays of $\tau_{\max} = 3T_c, 6T_c$, and $9T_c$, while having $L_p = 4$ delay spread-induced paths.

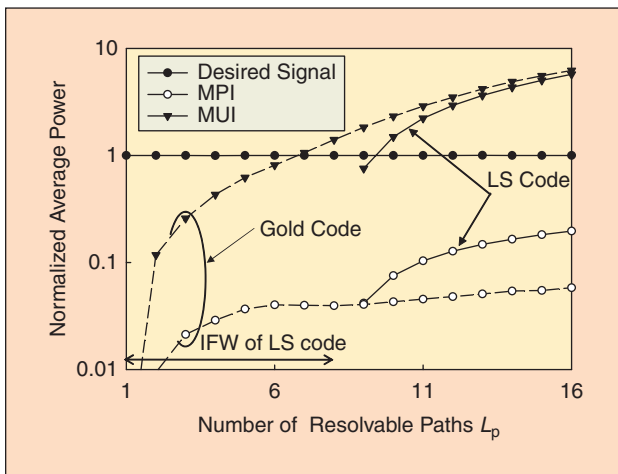


FIGURE 8 Effect of the number of resolvable paths L_p on the average power of the desired signal, on the MPI and on the MUI.

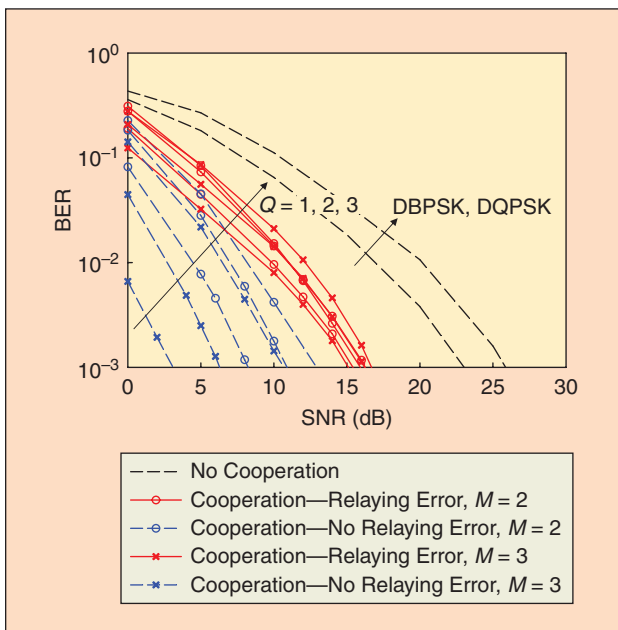


FIGURE 9 Achievable BER performance of our LS code-aided CDSTS scheme, employing $M = 2$ and 3 cooperating nodes for each source node, where the DLDC's multiplexing factor Q is changed from $Q = 1$ to $Q = 3$. We also plotted here the corresponding BER curves of our system suffering from no relaying errors, as well as those of noncooperative system having the modulations of DBPSK and DQPSK.

hand, for the high-delay scenarios of $\tau_{\max} = 6T_c$ and $9T_c$, where the sum of the maximum delay τ_{\max} and the delay spread $(L_p - 1)$ is higher than the LS code's IFW, the corresponding BER was substantially deteriorated because of the residual MUIs and MPIs, although it was still better than that of the Gold codes for any of the delays considered. To provide further insights, the BER curves associated with Gold codes of Figure 7 also correspond to the performance of the

conventional space-time coded cooperative schemes [2], which is typically affected by the relay nodes' synchronization errors as well as ISI. (To save the space economy, further comparisons with other cooperative schemes will be left for our future study.)

In Figure 8, we evaluated the effects of both the MPI and of the MUI during the cooperative phase-II, assuming that the number of resolvable paths L_p was varied from $L_p = 1$ to $L_p = 16$, while maintaining a maximum delay of $\tau_{\max} = 0$ for the sake of simplicity. We note here that the $(N_c \times M)$ relay nodes were quasi-synchronously transmitting their signals. Figure 8 shows the average powers of the desired signals, of the MPI and of the MUI, while comparing the performance of LS and Gold codes. First, it was confirmed that our LS code-aided CDSTS was capable of perfectly suppressing both the MUI and the MPI, provided that the delay-spread associated with the $(L_p - 1)$ delayed paths was within the designed IFW of W_0 , while the Gold code-aided system suffered from their residual MUI and MPI owing to the nonzero auto- and cross-correlations.

Finally, we investigated a more practical scenario, namely that of employing the shorter interleaver lengths of $\Pi_S = 2,000$ b and of $\Pi_R = 1,000$ b. Here we assumed quasi-static Rayleigh fading environments. Furthermore, the LS code of LS(8,16,7) was employed for the case of $M = 3$ relay nodes, to generate the required number of LS codes having an IFW of 7 chip durations. It is predicted that since no time diversity gain can be exploited in this block-fading scenario, the spatial diversity order, determined by the number of relay nodes, dominantly affects the preferable performance improvement. Hence, our multirelay-assisted DTC has the potential to exhibit a better performance than those of the conventional single-relay-assisted DTCs [8], [9], [11]. Figure 9 shows the achievable BER performance of our LS code-aided CDSTS scheme, employing $M = 2$ and $M = 3$ cooperating nodes, respectively, where the DLDC's multiplexing factor Q was varied from $Q = 1$ to $Q = 3$. Additionally, we plotted here the BER curves of our benchmark CDSTS system assuming the idealized scenario of having no decoding errors at the relay nodes, to benchmark the effects of the relays' decoding errors and their error propagation. Observe in Figure 9 that while the proposed CDSTS system achieved a better performance than the noncooperative scheme as a benefit of its cooperative spatial diversity gain, it was severely degraded by the relays' decoding errors, when compared with those of the no-relaying error scenario. Therefore, it was found that to exploit the designed diversity-multiplexing tradeoff, it is important to overcome the effects of error propagation by employing cyclic redundancy checks for the sake of identifying the relays' decoding errors, or by introducing the concept of [16], where the relays' decoding errors are

compensated for at the destination receiver by exploiting each relay's average BER estimated for the received LLRs. Furthermore, it can also be seen that upon increasing the number of relay nodes from $M = 2$ to $M = 3$, the potential diversity gain improves for each multiplexing factor Q , provided that the relays' decoding errors are successfully eliminated.

Generic Design Guidelines

The system design guidelines are summarized as follows:

- According to the degrees of the synchronization errors as well as the delay spread, the LS spreading codes assigned to the SNs and the RNs are designed so that the maximum delay becomes within the IFW.
- The DLDC's system parameters of (M, T, Q) as well as the modulation scheme are determined by the number of available RNs, the attainable diversity order between the RD link, and the normalized throughput.
- Then, the design of forward error correction (FEC) schemes employed at the SN and the RNs are optimized using two-dimensional EXIT charts, which accurately predicts the decoding behavior and threshold.
- Moreover, additional fundamental specification is the affordable decoding delay, which corresponds to the interleaver length, while a shorter interleaver degrades the achievable turbo-coding gain.
- To be more specific, when the desirable design criterion is achieving a near-capacity performance, rather than minimizing the overall delay and the decoding complexity, it is straightforward approach to match the inner- and outer-EXIT curves, hence attaining an infinitesimally low BER at near-capacity SNRs.

Further related techniques may be advocated into the above-mentioned cooperative system design.

Although the effects of MUI and MPI arriving within the IFW are perfectly eliminated in our cooperative system, the number of LS codes exhibiting a sufficiently wide IFW is limited. To extend the degree of design freedom and hence to accommodate large synchronous delays, multicarrier (MC) transmission can be invoked in our CDSTS system, as described in [7]. More specifically, the IFW duration of the LS codes can be extended by a factor given by the number of subcarriers, since the chip duration of each subcarrier is proportionately increased.

Conclusions

In this article, we proposed a practical cooperative transmission protocol, exploiting the advantages of asynchronous cooperation, noncoherent detection, and multirelay-assisted DTC. The DLDC scheme employed for our cooperative STC has the potential of adapting our CDSTS arrangement, such as the number of relay

THE IFW DURATION OF THE LS CODES CAN BE EXTENDED BY A FACTOR GIVEN BY THE NUMBER OF SUBCARRIERS, SINCE THE CHIP DURATION OF EACH SUBCARRIER IS PROPORTIONATELY INCREASED.

nodes and the transmission rate, depending on the network's topology and on the propagation environment encountered. Our simulation results demonstrated that the proposed LS code-aided CDSTS scheme is capable of achieving both cooperative spatial diversity and turbo-processing gains, while combating the effects of the relays' synchronization errors and CSI estimation errors. The family of space-time codes constitutes an efficient class of diversity techniques that are capable of combating the time-varying fading effects of wireless channels. Our multirelay-assisted DTC has the potential to exhibit a better performance than those of the conventional single-relay-assisted DTCs. The design of forward error correction schemes employed at the SN and the RNs are optimized using two-dimensional EXIT charts. The IFW duration of the LS codes can be extended by a factor given by the number of subcarriers, since the chip duration of each subcarrier is proportionately increased.

Acknowledgments

The financial support of the EU under the auspices of the Optimix project and of the EPSRC UK is gratefully acknowledged.

Author Information

Shinya Sugiura (sugiura@ieee.org) received his B.S. and M.S. degrees from Kyoto University, Japan, in 2002 and 2004, respectively, and his Ph.D. degree from the University of Southampton, United Kingdom, in 2010. Since 2004, he has been with Toyota Central R&D Laboratories, Inc., Japan. He authored/coauthored more than 45 refereed research publications, including 19 IEEE journal papers. He was awarded a number of distinctions, most recently, the 2011 Ericsson Young Scientist Award and the 2011 IEEE ComSoc Asia-Pacific Outstanding Young Researcher Award. He is a Senior Member of the IEEE. His research interests include wireless communications, networking, signal processing, and antenna design.

Soon Xin Ng (sxn@ecs.soton.ac.uk) received his B.Eng. degree (first class) in electronics engineering and Ph.D. degree in wireless communications from the University of Southampton, United Kingdom, in 1999 and 2002, respectively. From 2003 to 2006, he was a postdoctoral research fellow working on collaborative European research projects known

as SCOUT, NEWCOM, and PHOENIX. Since August 2006, he has been a member of the academic staff in the School of Electronics and Computer Science, University of Southampton. He is involved in the OPTIMIX European project, as well as IU-ATC and UC4G projects. He has published more than 120 papers and coauthored two Wiley/IEEE Press books. He is a Senior Member of the IEEE and a fellow of the Higher Education Academy in the United Kingdom. His research interests include adaptive-coded modulation, coded modulation, channel coding, space-time coding, joint-source and channel coding, iterative detection, OFDM, MIMO, cooperative communications, and distributed coding.

Lingkun Kong (lk06r@ecs.soton.ac.uk) received his B.Eng. degree in information engineering and M.Eng. degree in communications and signal processing from Southeast University, Nanjing, China, in 2004 and 2006, respectively. He is currently working toward his Ph.D. degree with the Communications Research Group, School of Electronics and Computer Science, University of Southampton, United Kingdom. His research interests include channel coding, space-time coding, iterative detection techniques as well as colocated and distributed MIMO systems.

Sheng Chen (sqc@ecs.soton.ac.uk) obtained his B.Eng. degree from the East China Petroleum Institute, Dongying, China, in January 1982, and his Ph.D. degree from City University, London, in September 1986, both in control engineering. In 2005, he was awarded the D.Sc. degree from the University of Southampton, United Kingdom. From 1986 to 1999, he conducted research and academic appointments at the Universities of Sheffield, Edinburgh, and Portsmouth, all in the United Kingdom. Since 1999, he has been with Electronics and Computer Science, the University of Southampton, United Kingdom, where he is currently a professor in Intelligent Systems and Signal Processing. He is a chartered engineer (C.Eng.) and a fellow of IET (FIET). He has published more than 450 research papers and is listed as a highly cited researchers in engineering. His recent research interests include adaptive signal processing, wireless communications, modeling and identification of nonlinear systems, neural network and machine learning, intelligent control system design, evolutionary computation methods, and optimization.

Lajos Hanzo (lh@ecs.soton.ac.uk) received his D.Sc. degree in electronics in 1976 and his doctorate in 1983. In 2009, he was awarded the honorary doctorate (Doctor Honoris Causa) by the Technical University of Budapest. Since 1986, he has been with the School of Electronics and Computer Science, University of Southampton, United Kingdom, where he holds the chair in telecommunications, and since 2009 he has been a

chaired professor at Tsinghua University, Beijing. He is directing a 100-strong academic research team, working on a range of research projects in the field of wireless multimedia communications sponsored by industry, the Engineering and Physical Sciences Research Council (EPSRC), United Kingdom, the European IST Programme, and the Mobile Virtual Centre of Excellence (VCE), United Kingdom. He has held various research and academic posts in Hungary, Germany, and the United Kingdom, and successfully supervised 80 Ph.D. students. He coauthored 20 Wiley/IEEE Press books on mobile radio communications totaling more than 10,000 pages, published more than 1,250 research papers, and has been awarded a number of distinctions. He was editor-in-chief of IEEE Press 2008-2012. He is a Fellow of the IEEE, IET, REng, and EURASIP, and a governor of VTS.

References

- [1] L. Hanzo, O. Alamri, M. El-Hajjar, and N. Wu, *Near-Capacity Multi-Functional MIMO Systems: Sphere-Packing, Iterative Detection and Cooperation* Hoboken NJ Wiley 2009 p. 714.
- [2] J. Laneman and G. Wornell, "Distributed space-time-coded protocols for exploiting cooperative diversity in wireless networks," *IEEE Trans. Inform. Theory*, vol. 49, no. 10, pp. 2415-2425, 2003.
- [3] P. Tarasak, H. Minn, and V. Bhargava, "Differential modulation for two-user cooperative diversity systems," *IEEE J. Select. Areas Commun.* vol. 23, no. 9, pp. 1891-1900, 2005.
- [4] R. C. Palat, A. Annamalai, and J. H. Reed, "Accurate bit-error-rate analysis of bandlimited cooperative OSTBC networks under timing synchronization errors," *IEEE Trans. Veh. Technol.* vol. 58, no. 5, pp. 2191-2200, 2009.
- [5] M. Sharp, A. Scaglione, and B. Sirkeci-Mergen, "Randomized cooperation in asynchronous dispersive links," *IEEE Trans. Commun.* vol. 57, no. 1, pp. 64-68, 2009.
- [6] Z. Li and X. Xia, "An Alamouti coded OFDM transmission for cooperative systems robust to both timing errors and frequency offsets," *IEEE Trans. Wireless Commun.*, vol. 7, no. 5(Pt. 2), pp. 1839-1844, 2008.
- [7] H. Wei, L. Yang, and L. Hanzo, "Interference-free broadband single- and multicarrier DS-CDMA," *IEEE Commun. Mag.*, vol. 43, no. 2, pp. 68-73, 2005.
- [8] M. Janani, A. Hedayat, T. Hunter, and A. Nosratinia, "Coded cooperation in wireless communications: space-time transmission and iterative decoding," *IEEE Trans. Signal Processing*, vol. 52, no. 2, pp. 362-371, 2004.
- [9] Y. Li, B. Vucetic, T. Wong, and M. Dohler, "Distributed turbo coding with soft information relaying in multihop relay networks," *IEEE J. Select. Areas Commun.*, vol. 24, no. 11, pp. 2040-2050, 2006.
- [10] L. Hanzo, T. Liew, and B. Yeap, *Turbo Coding, Turbo Equalisation, and Space-Time Coding for Transmission over Fading Channels* Hoboken NJ: Wiley, 2002, p. 766.
- [11] S. Ng, Y. Li, and L. Hanzo, "Distributed turbo trellis coded modulation for cooperative communications," in *Proc. IEEE Int. Conf. Communications*, Dresden, Germany, June 2009, pp. 1-5.
- [12] B. Hassibi and B. Hochwald, "Cayley differential unitary space-time codes," *IEEE Trans. Inform. Theory*, vol. 48, no. 6, pp. 1485-1503, 2002.
- [13] S. ten Brink, "Convergence behavior of iteratively decoded parallel concatenated codes," *IEEE Trans. Commun.*, vol. 49, no. 10, pp. 1727-1737, 2001.
- [14] D. Divsalar, S. Dolinar, and F. Pollara, "Serial concatenated trellis coded modulation with rate-1 inner code," in *Proc. IEEE Global Telecommunications Conf.*, Nov.-Dec. 2000, vol. 2, San Francisco, CA, pp. 777-782.
- [15] B. Hochwald, T. Marzetta, and C. Papadias, "A transmitter diversity scheme for wideband CDMA systems based on space-time spreading," *IEEE J. Select. Areas Commun.*, vol. 19, no. 1, pp. 48-60, 2001.
- [16] K. Lee and L. Hanzo, "Optimal decoding for hard-decision forwarding aided cooperative spatial multiplexing systems," *IEEE Trans. Wireless Commun.*, vol. 8, no. 9, pp. 4411-4416, 2009.

VT